

Static Permeability of AL-800 Garnet Material

R. Madrak, G. Romanov, and I. Terechkin

To correctly evaluate losses in a tunable RF cavity, one must have detailed knowledge of static magnetization curve of YIG material. This note describes a setup for corresponding magnetic measurements and results of our attempts to extract the saturation curve of AL-800 material from the data obtained by the measurements.

AL-800 material sample is placed inside existing solenoid designed by V. Kashikhin and A. Makarov for RF tuners at AD. A sketch of the setup is shown in Fig. 1.

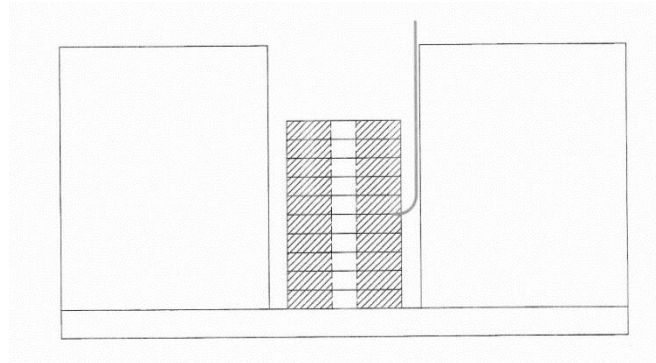


Fig. 1. Setup concept for measurements of static magnetization.

Main dimensions and other parameters of the solenoid are as following: the length of the coil is 177.8 mm, inner diameter is 100.0 mm, and the outer diameter is 305.0 mm. The nominal number of turns in the coil $N = 112$. The magnet was designed with the flux return built using CDM-10 ferrite, but at least part of the flux return used G4 material instead; the difference in the materials does not play significant role though. The inner diameter of the flux return is 320 mm, thickness is 20 mm, and the diameter of the hole in the top plate is 105 mm.

Magnetic properties of the CDM-10 ferrite are shown in the table below and illustrated by corresponding figure. The material was formulated to have higher permeability at higher field.

B (G)	mu
10	550
20	570
100	650
300	950
1000	1750
2000	2500
2700	2950
3000	2980
3300	2950
4000	1800
5000	200
6000	20
10000	1.75

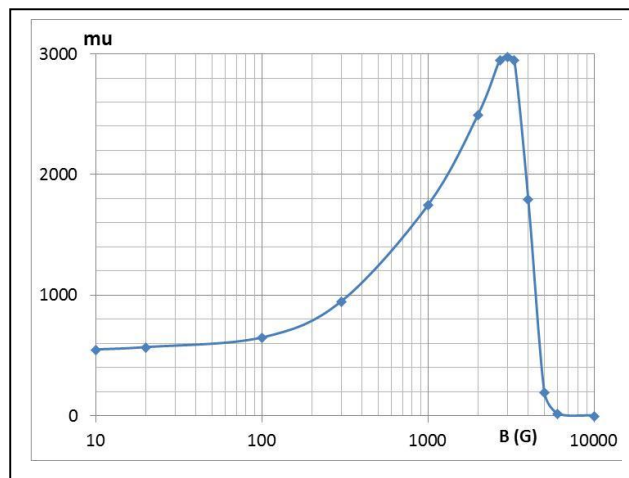


Fig. 2. Magnetic properties of CMD-10 material.

The AL-800 material sample is assembled of ten rings, 12.7 mm (0.5”) thick each, placed symmetrically inside the solenoid. The inner diameter of the rings is 16.51 mm, and the outer diameter is 76.2 mm. The geometry of the sample is shown in Fig. 3. Saturation magnetization of the YIG material $M_s = 63662[A/m]$ (800 Oe).

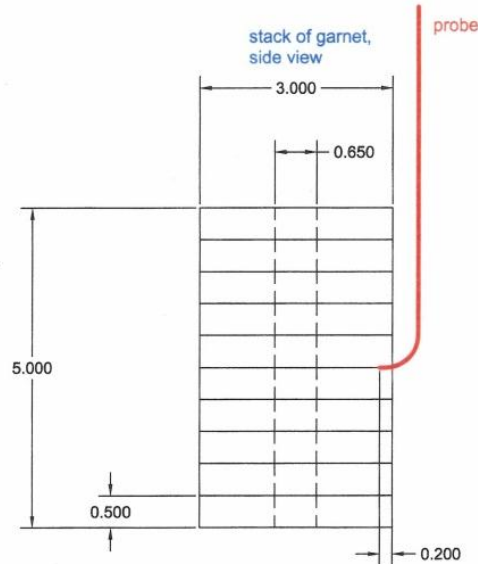


Fig. 3. Geometry of the material sample. Dimensions are in inches.

As static magnetization curve of the sample material was found using iterative process, initial assumption about the permeability as a function of magnetic field was used to start the iterations. For example, this “zero iteration” function can look like shown in Fig. 4.

B(T)	mu_static
0	50
0.05	49.7
0.07	46.5
0.08	25
0.09	9
0.1	5
0.12	3
0.14	2.3
0.16	2
0.2	1.66
0.25	1.47
0.3	1.36
0.35	1.3

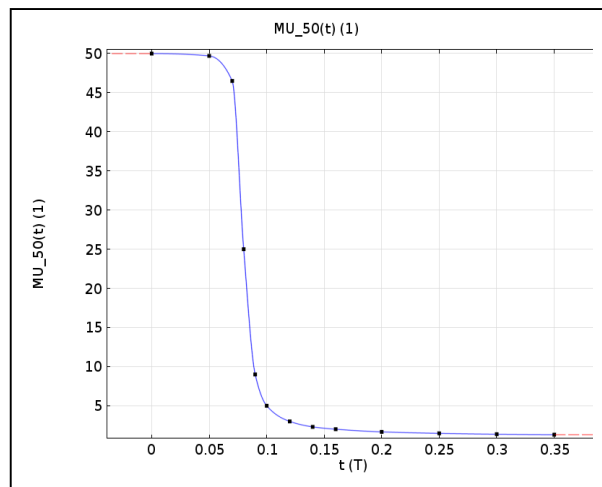


Fig. 4. Assumed zero-iteration magnetic properties of the AL-800 material

This curve was obtained by using the maximum initial permeability (that is at $B = 0$) of ~ 50 (according to available vendor’s data and information found in other publications) and using a theoretical RF permeability for $B > 800$ G. Between zero and 800 G, the curve is essentially

imagined. The goal of this work was computationally reproduce results of magnetic field measurements in the sample in Fig. 3 with the setup shown in Fig. 2 using iteratively adjusted magnetization curve, starting from the initial approximation.

Three magnetometers were available for the measurement; they were cross-calibrated in the magnet in the current range from 0 to 80 A. Three Hall probes were installed: in the center of the solenoid, between the rings #1 and #2, and between the rings #9 and #10. Readings of the probes were taken at several current levels. Results of the measurements were compared with modeling using iterative approach: the magnetization curve was gradually changed starting with low current. At each new current level, changes to the magnetization curve used at the previous level were made until the modeling result properly reflected the measurement data.

Three attempts of extracting the magnetization curve out of data obtained by measurements were made. During the first attempt (end of January 2015), the readings of the AphaLab magnetometer (calibrated by the vendor on January 26) were used as the reference; readings of other two magnetometers were adjusted correspondingly by using cross-calibration. This resulted in some correction for the number of turns in the coil: 110 instead of nominal 112. This correction was not supported by the data in corresponding traveler document that claimed that the number of turns is 112.

Next, an attempt to calibrate the magnetometers was made using existing (in IB-1) magnet. As a base for the calibration a Hall probe magnetometer was used that was considered sufficiently precise. The data obtained during the first measurement session was recalculated – it resulted in the increase of the number of turns to 113, which was a good sign. Nevertheless, the attempt to find the sample material magnetization curve was not tremendously successful as the changes made to fit higher current data led to deterioration of the fit for the lower current. So, the process did not converge as desired.

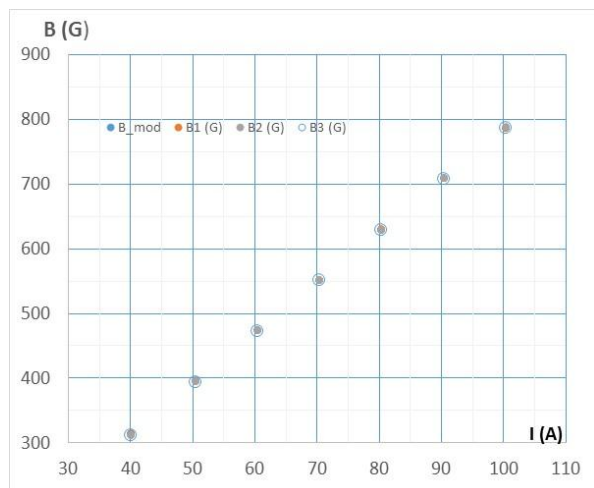
At this point it was decided to repeat the measurements using a better quality set of the rings, assuming $N = 112$, and using our magnetic system as a calibration stand. Readings of the three magnetometers were adjusted based on calculated values of the field at the location of the probes. This calibration resulted in the following correction factors for the used magnetometers ($k = \text{reading/modeling}$):

For the Cryomagnetics meter $k_1 = 1.075$;

For the AlphaLab magnetometer $k_2 = 1.016$;

For the DELL magnetometer $k_3 = 0.94$.

After applying these coefficients, comparison of the readings and the modeling at several currents is shown in Fig. 5. Corresponding set of data is also shown below.



I (A)	B_mod	B1 (G)	B2 (G)	B3 (G)
0	0	0	0	0
40.07	313.47	312.37	311.32	311.70
50.54	395.36	394.23	395.28	393.62
60.51	473.34	472.74	473.92	472.34
70.42	550.92	550.88	551.18	550.53
80.39	628.90	629.12	628.94	628.72
90.51	708.05	708.28	708.66	707.45
100.47	786.03	786.33	787.40	786.17

Fig. 5. Reading of the probes after application of the correction coefficients.

During the measurement, the sample was installed in two positions:

Position 1: data with the probes installed as following:

- Cryomagnetism magnetometer at the bottom;
- AlphaLab magnetometer in the middle;
- DELL magnetometer at the top.

Position 2: data with the probes installed as following

- Cryomagnetism magnetometer at the top;
- AlphaLab magnetometer in the middle;
- DELL magnetometer at the bottom.

Data collected in the two positions is shown below:

	U (mV)	I (A)	Raw Data		
			B1 (G)	B2 (G)	B3 (G)
1	39	1.95	184.1	154.6	86.2
2	88	4.41	416.5	350	193.8
3	128	6.41	595.4	502.5	277
4	155	7.76	685	585	326
5	201	10.07	771	673.2	388
6	244	12.22	819.5	728.3	435
7	283	14.17	851.8	765.5	474
8	322	16.13	877.5	792	510
9	357	17.88	898.3	813.6	541
10	397	19.88	920	836	575
11	519	26.00	980.8	895.5	665
12	604	30.25	1020.9	932.8	715
13	708	35.46	1068.5	977.5	768
14	800	40.07	1109.8	1015.8	807
15	901	45.13	1154.8	1057.7	847
16	1012	50.69	1203.6	1103	889
17	1119	56.05	1250.7	1146	928
18	1214	60.81	1292.2	1184.5	964
19	1302	65.21	1330.9	1221	996
20	1400	70.12	1373.6	1259.3	1031
21	1495	74.88	1415.1	1298.5	1065
22	1605	80.39	1462.9	1342.3	1105
23	0	0	9.5	7	1

a)

	U (mV)	I (A)	Raw Data		
			B1 (G)	B2 (G)	B3 (G)
1	36	1.95	98.9	145	138
2	79	4.41	214.5	315.3	301
3	121	6.41	328.3	428.7	457
4	161	7.76	415.5	604	580
5	195	10.07	471	669.8	642
6	238	12.22	529.5	728.2	692
7	280	14.17	578.9	769	726
8	323	16.13	623.3	800	753
9	360	17.88	658.1	822.5	773
10	400	19.88	693.5	844.7	793
11	500	26.00	771.1	894.5	838
12	604	30.25	838.1	940.5	881
13	699	35.46	889.9	982	919
14	800	40.07	938.1	1023	959
15	904	45.13	984.3	1068	999
16	1002	50.69	1026.3	1109	1037
17	1106	56.05	1070.3	1151.5	1077
18	1201	60.81	1110.2	1190.5	1113
19	1302	65.21	1152.1	1232	1151
20	1401	70.12	1193.2	1272.4	1188
21	1507	74.88	1237.2	1315.7	1229
22	1602	80.39	1276.4	1354.4	1264
23	0	0	8	10	6

b)

Fig. 6. Readings of the probes during the current scan: a) position 1; b) position 2.

As in the two positions the probes of different magnetometers exchange their locations, after application of the correction factors (drift and calibration corrections), the adjusted readings for the same location must coincide. The extent to which this statement is valid is reflected by the two tables below; the table on the right was adjusted to the current points of the left table by using linear interpolation.

k1	k2	k3			k1	k2	k3
1.075	1.016	0.94			1.075	1.016	0.94
Corrected for Readings				Corrected for Readings & Current			
Bottom	Mid	Top	I (A)	Top	Mid	Bottom	
B1 (G)	B2 (G)	B3 (G)		B1 (G)	B2 (G)	B3 (G)	
170.87	151.87	91.66	1.95	99.16	153.95	158.61	
386.67	343.89	206.08	4.41	221.50	333.30	355.16	
552.71	493.69	294.54	6.41	318.56	450.78	508.19	
635.67	574.59	346.62	7.76	376.16	581.42	604.32	
715.29	661.10	412.53	10.07	444.07	665.07	688.97	
760.02	715.03	462.49	12.22	497.14	719.84	739.63	
789.68	751.35	503.93	14.17	539.11	755.99	772.38	
813.21	777.13	542.18	16.13	576.36	783.39	798.28	
832.17	798.09	575.12	17.88	606.83	804.09	818.27	
851.97	819.84	611.24	19.88	639.72	825.66	839.41	
908.15	878.10	706.94	26.00	725.07	883.90	896.74	
945.06	914.52	760.08	30.25	775.75	920.55	933.90	
988.96	958.21	816.42	35.46	827.57	964.53	977.82	
1026.99	995.61	857.86	40.07	868.12	1000.90	1016.33	
1068.47	1036.55	900.37	45.13	909.59	1043.54	1057.37	
1113.48	1080.84	945.00	50.69	953.43	1088.67	1102.82	
1156.91	1122.86	986.45	56.05	995.16	1131.29	1146.23	
1195.13	1160.45	1024.70	60.81	1031.90	1169.25	1184.21	
1230.75	1196.08	1058.70	65.21	1065.57	1204.47	1219.20	
1270.08	1233.48	1095.88	70.12	1103.10	1243.41	1257.87	
1308.30	1271.76	1132.01	74.88	1139.52	1281.24	1296.95	
1352.38	1314.57	1174.51	80.39	1181.00	1325.00	1340.00	

Averaged values of the field for the three locations of the probes will be used for further work. The maximum deviation from the average reaches ~4% for the top location, where the field is quite non-uniform, and for low current level. It is ~0.5% for the current exceeding ~25 A. Table and graph in Fig. 7 show the data that will be used as a starting point for further work.

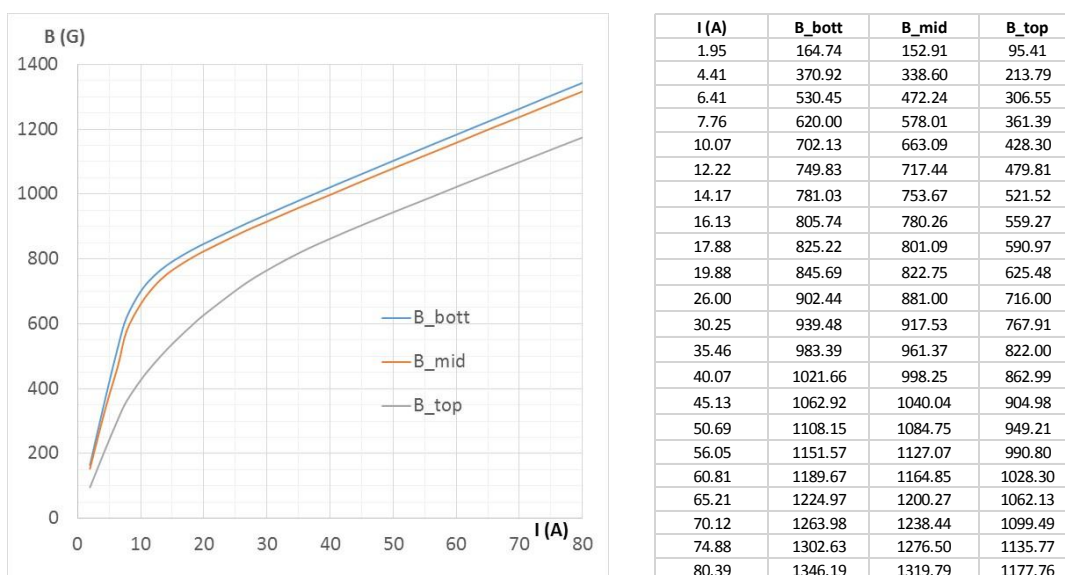


Fig. 7. Readings of the probes at the bottom, in the middle and at the top of the sample.

Modeling shows that at small current (up to $I \approx 5$ A) permeability is constant everywhere. It is 50 for the “zero” iteration permeability in Fig. 4, so the permeability map in Fig. 8 shows quite uniform field. Hence, we can use a constant value to check how it fits to the results. Measuring the field in the gap at low current and choosing the value of μ in the model that gives the same field value allows obtaining the value of initial permeability μ_{init} .

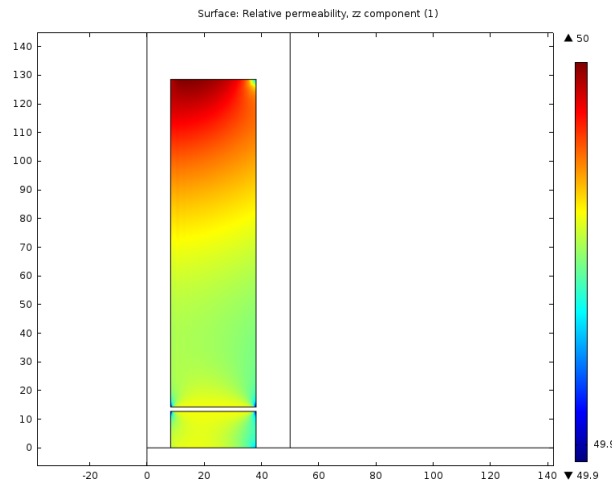


Fig. 8. Permeability of the sample at low current

The presence of the gaps makes significant impact on the field distribution. Figure below compares the field at the same current (2.5 A) along the line $R = 23$ mm without any gaps and with three gaps. The gaps were carefully measured and 1.37 mm gap width was accepted during this modeling session.

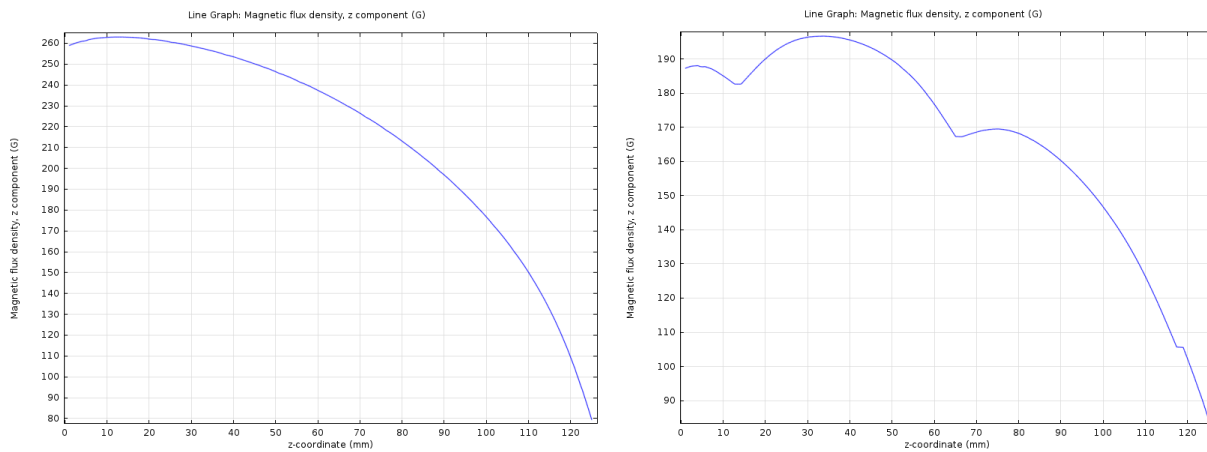


Fig. 9. The impact of the gaps in the sample.

After a number of iterations of the fitting process a permeability curve was found (Figures 10 and 11) that satisfactory fits all the measurement data. Corresponding data tables are also shown below.

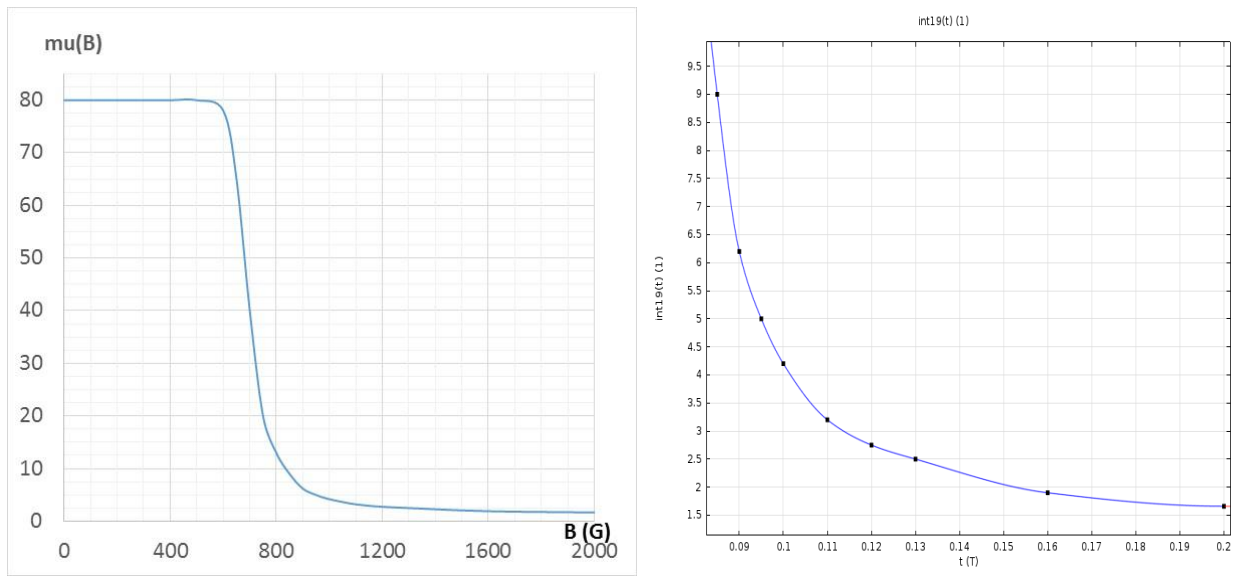


Fig. 10. Magnetization curve in the form $\mu(B)$

B (G)	mu
0	80
100	80
200	80
300	80
400	80
500	80
600	78
650	65
700	40
750	20
800	13
850	9
900	6.2
950	5
1000	4.2
1100	3.2
1200	2.75
1300	2.5
1600	1.9
2000	1.66

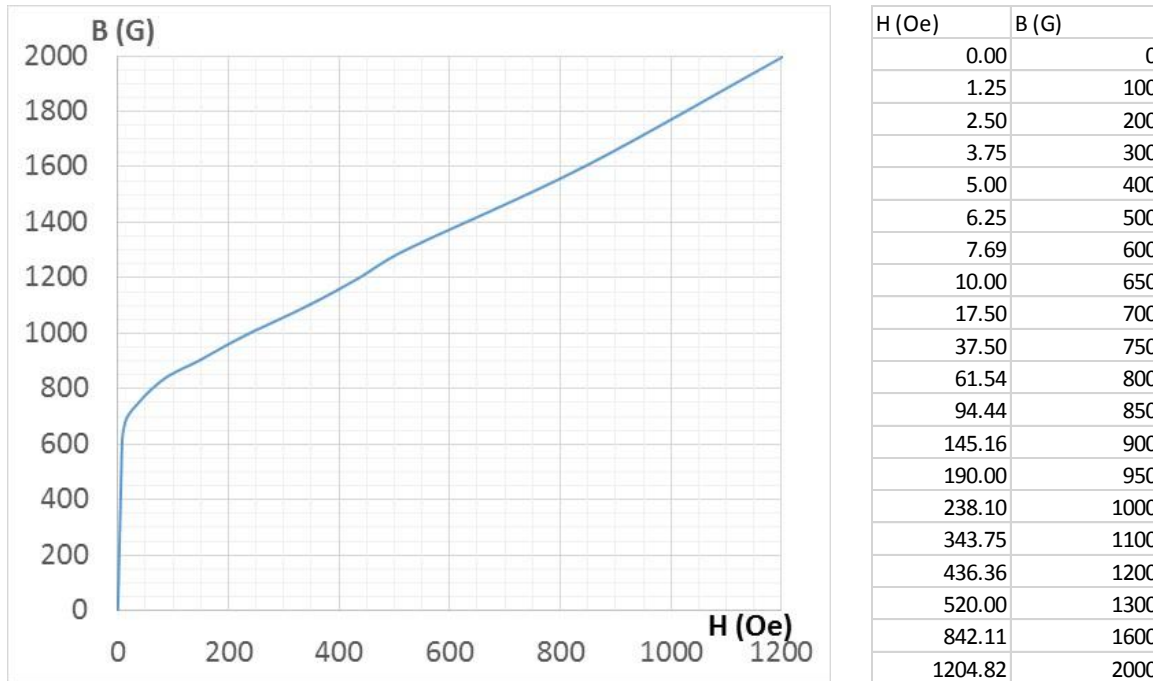


Fig. 11. Magnetization curve in the form B(H)

A table that compares the measured and modeled values of the probes' readings is shown below.

I (A)	bott_model	bott_meas	mid_model	mid_meas	top_model	top_meas
4.41	363.3	353.2	330.6	326.7	206.6	202.5
7.76	628.8	625.8	572.4	583.7	358.4	365.9
10.07	705.2	698.4	663.2	659.1	428.4	424.5
12.22	746.1	747.3	714.4	714.6	480	476.6
16.13	807.5	806.0	782	780.6	563.3	559.7
19.88	846.1	846.4	826.2	823.48	626.8	626.6
30.25	935.5	939.5	918.5	917.5	759.5	768
40.07	1016.5	1021.66	1001.1	998.3	850	863
50.69	1096.6	1106.1	1081	1082.7	931.5	947.3
60.81	1182.5	1187.1	1164.5	1162.4	1007	1025.8
80.39	1356.4	1345.5	1336.8	1319.1	1156	1177.4

This table is illustrated by the graph in Fig. 12.

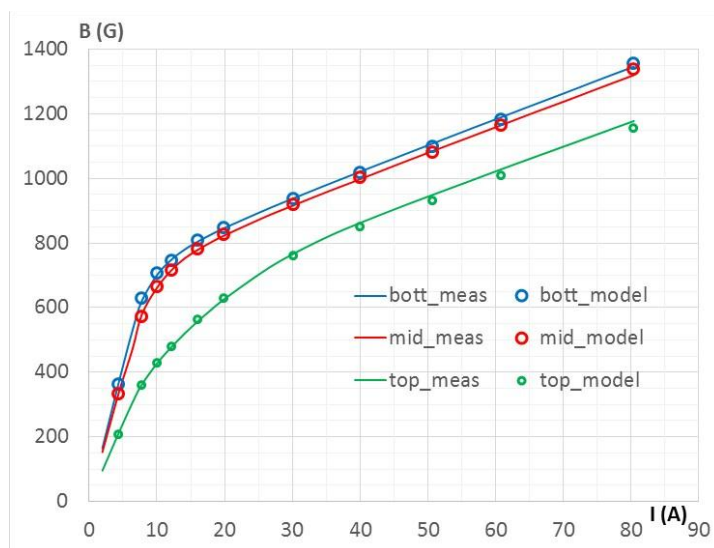


Fig. 12. Comparison of the data obtained by the measurements with that obtained by the modeling using the found magnetization curve.

Data obtained by magnetic measurements with three probes was used to synthesize a magnetization curve of the YIG material with the help of iterative modeling. Although intermediate results of the probes' cross-calibration point to satisfactory accuracy of the measurements, the non-uniformity of the field in the sample material can lead to some uncertainty especially in the low current region. To improve the uniformity, modification of the test setup is required by using an additional pole in the top portion of the magnet; this can improve precision of the results in the low current region.

Figures below compare two cases: with and without steel pole insert. One can see that adding an additional pole to the system significantly improves the uniformity of the field. This will make the job of fitting the magnetization curve much more straightforward.

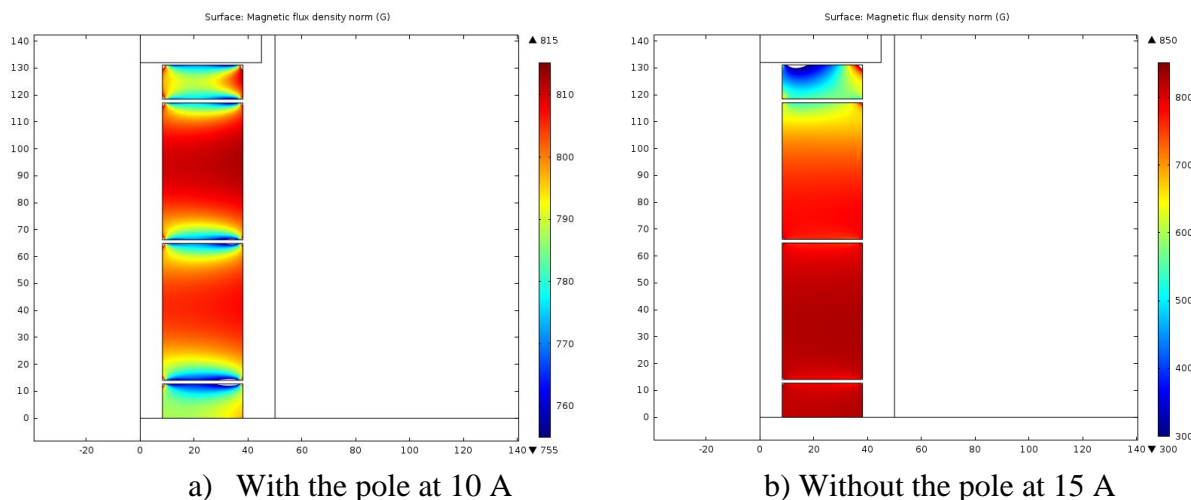


Fig. 13. Field in the stack with and without additional ferromagnetic pole.

The same three probes were used, but position of the probes was changed: the probe of the AlphaLab magnetometer was at the bottom, the probe of the Cryomagnetics magnetometer was placed in the middle, and the DELL magnetometer was used to measure the field at the top. The steel pole was placed directly on the top of the stack of the AL800 discs. The table and the figure below illustrates the measurement data. The same figure shows data points obtained by the modeling.

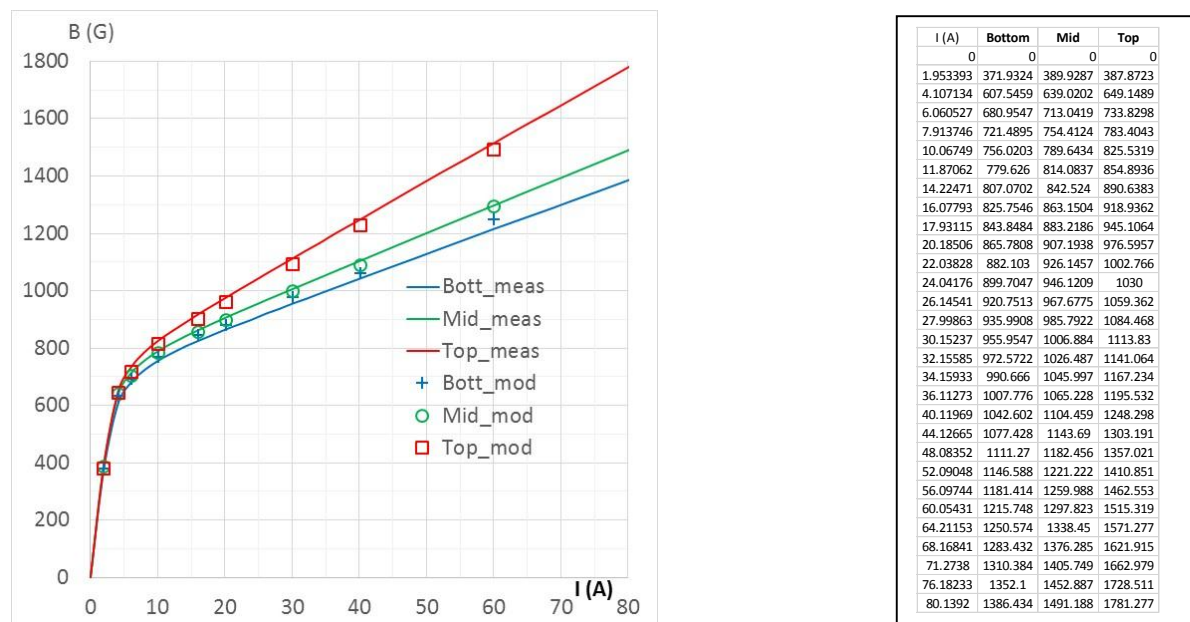


Fig. 14. Data obtained during the measurement session with the steel pole and fitting results.

As earlier, we started the search of a new magnetization curve using constant permeability at low current. Satisfactory data was obtained only using $\mu = 150$. The magnetization curve found in the previous attempt was modified correspondingly, and after several iterations of adjusting intermediate part of the curve (in the area approximately corresponding to the saturation magnetization), the next approximation was obtained:

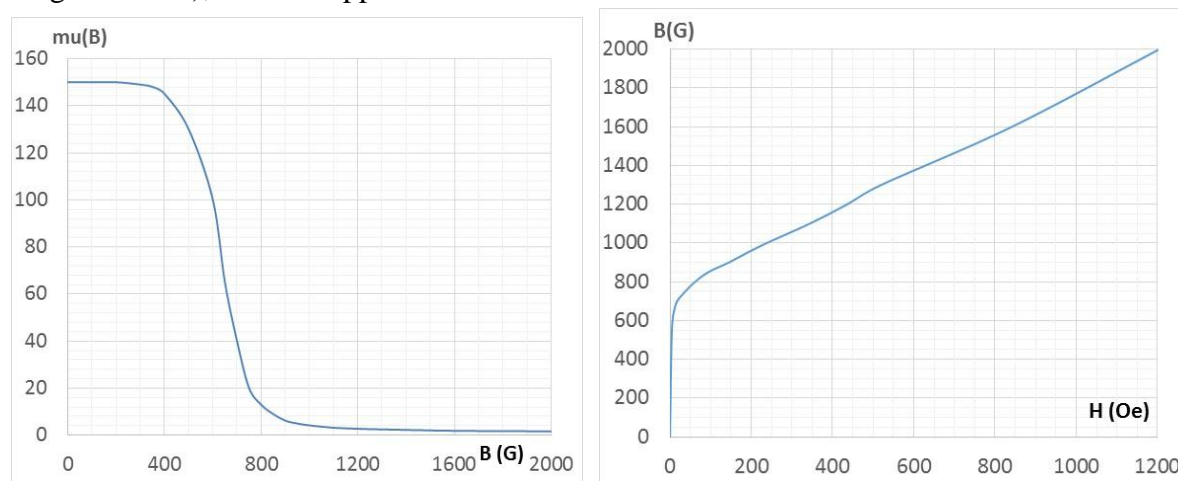


Fig. 15. Magnetization curve obtained with the use of a steel pole.

Corresponding table is shown below:

H (Oe)	B(G)	mu(B)
0.00	0	150
0.67	100	150
1.33	200	150
2.01	300	149
2.36	350	148
2.76	400	145
3.85	500	130
6.00	600	100
10.00	650	65
17.50	700	40
37.50	750	20
61.54	800	13
94.44	850	9
145.16	900	6.2
190.00	950	5
238.10	1000	4.2
343.75	1100	3.2
436.36	1200	2.75
520.00	1300	2.5
842.11	1600	1.9
1204.82	2000	1.66

It worth to mention that the difference between the magnetization curves plotter in Fig. 11 and Fig. 15 and obtained during the two iterations we made is undistinguishable for the field levels above ~10 Oe. Below 10 Oe, the new curve is characterized by higher tangent resulting from higher permeability (Fig. 17).

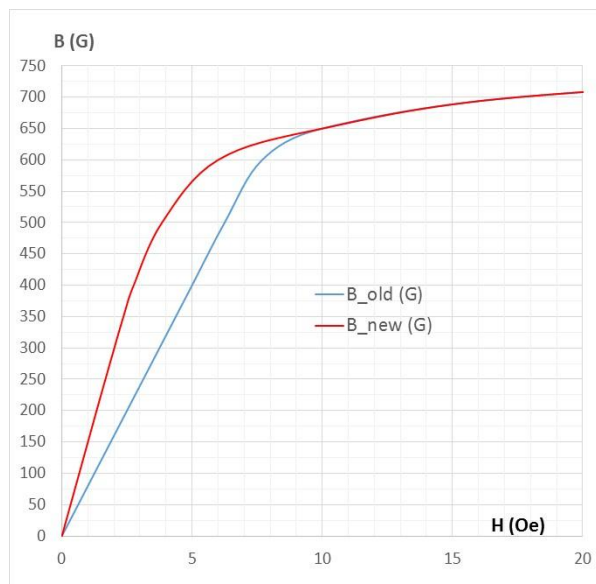


Fig. 17. Comparison of the magnetization curves obtained during two measurement sessions.

Summary.

By comparing results of magnetic measurements made using sample AL800 material with results obtained by modeling, we were able to refine our understanding of the static magnetic properties of the material (magnetization curve).

Using the known static magnetic properties while analyzing results of RF measurements on a cavity filled with AL800 material in the presence of magnetic field (in progress) allows us to get reliable data to define complex RF permeability.

This knowledge will serve as a starting point for the final stage the tunable cavity design.